Chemistry & Biology, Vol. 11, 487–498, April, 2004, ©2004 Elsevier Science Ltd. All rights reserved. DOI 10.1016/j.chembiol.2004.03.023

# Poly(β-amino ester)s Promote Cellular Uptake of Heparin and Cancer Cell Death

**David Berry,[1,2,3] David M. Lynn,[4] Ram Sasisekharan,[2,3,5] and Robert Langer[2,3,4,*]**
[1]Harvard Medical School
Boston, Massachusetts 02215
[2]Harvard-Massachusetts Institute of Technology
Division of Health Sciences and Technology
Cambridge, Massachusetts 02139
[3]Division of Biological Engineering
[4]Department of Chemical Engineering
[5]Center for Biological Engineering
Massachusetts Institute of Technology
Cambridge, Massachusetts 02139

## Summary

**Heparin/heparan sulfate-like glycosaminoglycans (HSGAGs) are involved in diverse cellular processes in the extracellular matrix (ECM). The biological effect of HSGAGs depends on disaccharide content and physiological location within the ECM. HSGAGs are also brought into cells during membrane transcytosis and growth factor signaling while protein bound. We sought to probe the impact of free HSGAGs within the cell by using heparin as a model HSGAG. A library of poly(β-amino ester)s, which internalize DNA, was examined for the capacity of its members to internalize heparin. Fourteen polymers enabled heparin internalization. The most efficacious polymer reduced murine melanoma cell growth by 73%. No glycosaminoglycan was as efficacious as highly sulfated, full-length heparin. Internalized heparin likely interferes with transcription factor function and subsequently induces apoptotic cell death. Therefore, internalized heparin is a novel mechanism for inducing apoptosis of cancer cells.**

## Introduction

The role of heparin/heparan sulfate-like glycosaminoglycans (HSGAGs) in influencing biological processes has been defined by their function in the extracellular matrix (ECM). HSGAGs are found as the glycosaminoglycan (GAG) component of heparan sulfate proteoglycans (HSPGs). Depending on the core protein, HSPGs are either free in the ECM or at the cell-ECM interface [1]. Interactions between HSGAGs and other ECM components regulate important physiological and pathological processes, including normal development, wound healing, and tumor progression [2, 3].

HSGAGs can regulate such a wide variety of cell processes because of their information-rich nature [4]. The HSGAG polysaccharide is composed of a disaccharide repeat unit consisting of a glucosamine linked to either an iduronic acid or a glucuronic acid. Potential 2-O sulfation on the uronic acid, 6-O and 3-O sulfation of the glucosamine, and an unmodified, acetylated, or sulfated amine lead to 48 potential disaccharide units that compose the 10–100-mer HSGAG chain [2]. In addition to the information content inherent in the polysaccharide chain [5], the relative biological location of both the HSGAG and the HSPG influences function. The tumorigenicity of an HSGAG chain is distinct whether it is free in the ECM or attached to an HSPG on the cell surface [6].

In normal function, HSGAGs are brought into the cell in a controlled fashion. For example, HSGAGs bind to fibroblast growth factor (FGF) 2 and FGF receptor (FGFR) 1 to form an internalized ternary complex [7, 8]. HSGAGs may facilitate the localization of the FGF-FGFR-HSGAG complex to the nucleus, where it impacts cell function [9]. Nonetheless, the role of free HSGAGs within the cell has not been established. Poly(β-amino ester)s (PAEs) are a class of cationic polymers that bind to DNA and enable its internalization by endocytosis [10, 11]. The low toxicity of this set of polymers compared to other cationic polymers that can also bind and internalize DNA, including poly(lysine) and poly(ethylene imine) [10, 12], provides an optimal method for investigating the potential for the internalization of HSGAGs with heparin as a model HSGAG, as well as a useful tool for understanding the effects of free HSGAGs within the cell.

The capacity of the PAEs to bind DNA and enable internalization, presumably by forming a conjugate with a net positive charge to promote endocytosis [10, 13], makes heparin binding and internalization rational. Herein, we investigated the capacity of PAEs to bind and internalize heparin, as well as the resultant cellular effects. We found that, although most polymers can bind heparin, only a small subset enables efficient internalization. Entry of heparin into cells promotes cell death, which is limited primarily by the rate at which cells internalize the polymer-heparin conjugate. The magnitude of cell death is maximal with PAEs conjugated to heparin rather than to other GAGs. We found that internalized heparin promotes spermine influx, a general increase in transcription factor levels in both the nucleus and cytosol, and apoptotic cell death.

## Results

### PAEs Bind Heparin

PAEs have been previously demonstrated to efficiently bind DNA [10, 11]. The interaction between this class of polymers and DNA is thought to be primarily mediated through electrostatic interaction between the anionic DNA and the cationic polymers. azure A is a cationic dye that binds to sulfate groups on heparin [14]. We examined polymer-heparin binding by determining if polymers could compete with azure A for binding sites on heparin. The ability of PAEs to displace Azure A was initially examined for five polymers with variable DNA binding efficiencies over a range of polymer:heparin

*Correspondence: rlanger@mit.edu

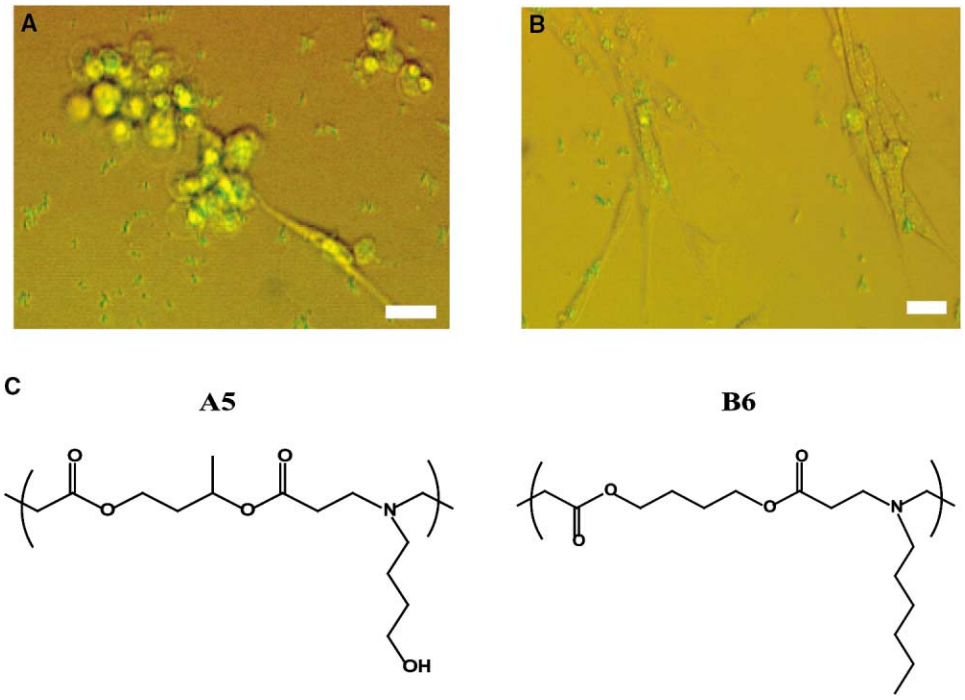


Figure 1. Select PAEs Enable Internalization of Heparin

(A and B) SMCs were incubated with conjugates of fluorescein-labeled heparin and various polymers. Fluorescence microscopy images of polymers (A) A5 and (B) B6 are shown. Images are presented as an overlay of fluorescence onto light microscopy. Scale bars represent 10 μm. (C) Polymers A5 and B6.

(w/w) ratios. All five polymers displaced heparin. The optimal ratios for these five polymers were at either 5:1 or 20:1. The 70 PAEs that had been previously demonstrated to be water soluble from an initial screening group of 140 [11] were then tested for their ability to bind heparin. Of the 70 polymers tested, 64 bound heparin to some degree at a 5:1 (w/w) polymer:heparin ratio, and all 70 bound heparin at a 20:1 ratio in 25 mM sodium acetate. When dissolved in phosphate-buffered saline (PBS), only 57 polymers bound heparin at a 5:1 (w/w) ratio, and 63 did so at a 20:1 (w/w) ratio. pH affects not only the rate at which PAEs degrade but also their ability to directly bind DNA [10]. The reduced ability of PAEs to bind heparin at a higher pH is consistent with DNA's reduced ability to do so.

### Select PAEs Enable Internalization of Heparin

To determine if PAE binding to heparin would enable internalization into cells, as is the case for PAE-DNA conjugates [10, 11], we employed fluorescein-labeled heparin. Conjugates of polymer and fluorescein-labeled heparin were formed in 25 mM sodium acetate for each of the 70 water-soluble polymers at a 20:1 (w/w) polymer:heparin ratio. The conjugates were incubated with smooth-muscle cells (SMCs), bovine aortic endothelial cells (BAECs), and NIH 3T3 cells for 24 hr, and internalization was detected by fluorescence microscopy. A group of 14 polymers composed of diacrylate "A" and amine "5" (A5), A8, A11, B6, B9, B11, B14, C4, C12, D6, E7, E14, F20, and G5 (Figure 1) enabled passage of heparin across the cell membrane; this heparin passage sufficiently met the criteria detailed in Experimental Procedures. The structures of A5 and B6 can be seen in Figure 1C. The chemical properties of the various polymers examined and the complexes formed with them have been reported previously [11, 15].

### Internalized Heparin Inhibits B16-F10 Growth

We treated B16-F10 cells with polymer-heparin complexes to investigate if internalized heparin could influence cell processes. Polymer-heparin complexes were formed at a polymer:heparin ratio of 20:1 (w/w) with each of the 14 polymers that enabled heparin internalization. Cells were treated with enough complexes to produce a heparin concentration of 500 ng/ml. Internalization of heparin caused a polymer-specific and polymer-dependent response in terms of B16-F10 proliferation (Figure 2A). A5-heparin induced a 58.28% $\pm$ 12.97% reduction in cell number in treated versus untreated cells; this reduction was significantly greater than that induced by any other polymer-heparin conjugate tested ($p < 0.008$). Heparin alone inhibited cell growth 2.40% $\pm$ 10.33%.

To examine whether the observed conjugate-induced effects were related to FGF2 cell-mediated responses, we added each of the 14 polymer-heparin complexes and 10 ng/ml FGF2 to the cells. In the presence of FGF2, A5-heparin reduced the whole-cell number by 86.51% $\pm$ 1.05% in treated compared to untreated cells. Given that FGF2 alone produced a 26.28% $\pm$ 7.23% inhibition, the increased magnitude of the inhibitory effect appears to be additive (Figure 2B). FGF2 generally promoted inhibition across polymers in an additive manner. D6 provides a notable exception in that cell number inhibi-

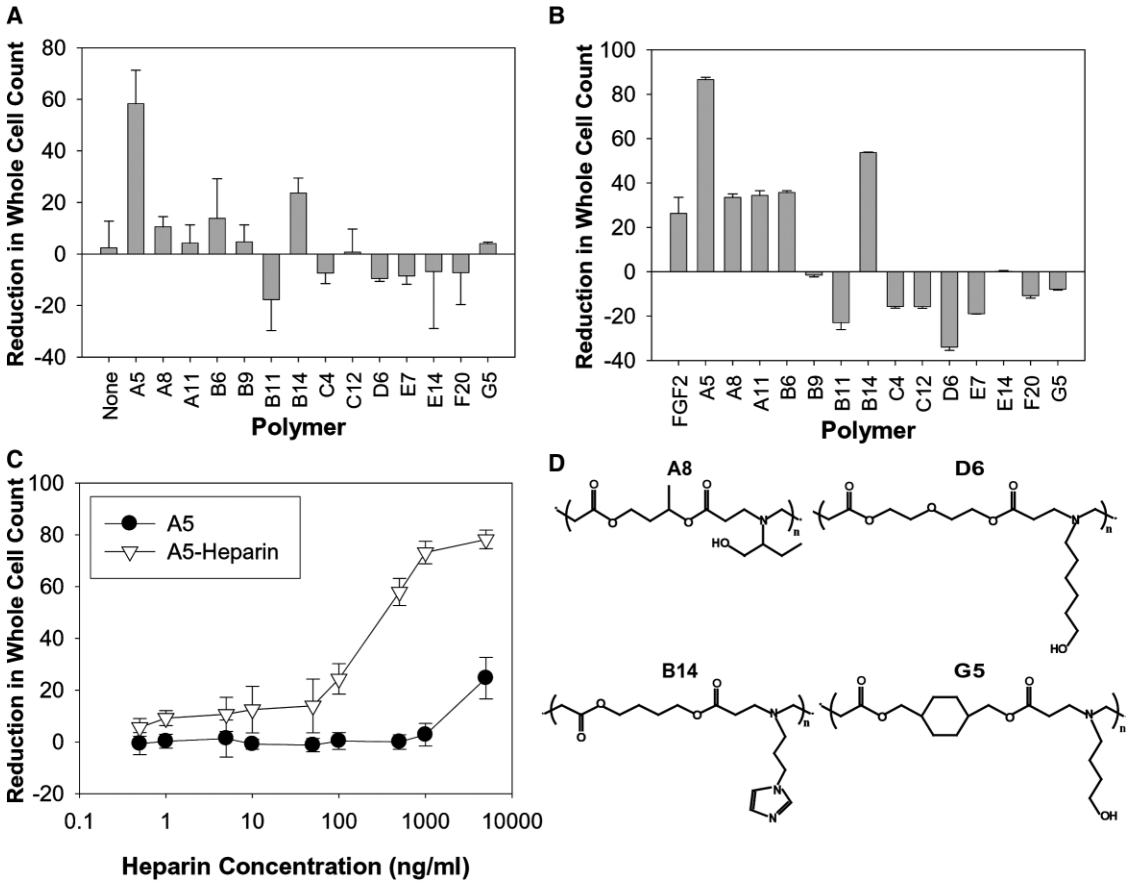


Figure 2. A5-Heparin Reduces B16-F10 Growth

B16-F10 cells were treated with polymer-heparin conjugates (A) alone or (B) with 5 ng/ml FGF2. Data were normalized as percent reduction in the whole-cell count compared to untreated cells. (C) B16-F10 cells were treated with A5-heparin at a 20:1 (w/w) ratio or with equivalent amounts of A5 alone. The whole-cell count was converted to a percent reduction compared to that of untreated cells. (D) Chemical structures of four polymers that had notable cellular effects after conjugation to heparin.

tion *decreased* from −9.51% ± 1.13% to −33.97% ± 1.47%.

We next examined the dose dependence of A5-heparin. The capacity of A5-heparin conjugates to reduce the whole-cell number increased with concentration (Figure 2C). The addition of 5 μg/ml heparin and 100 μg/ml A5 reduced the whole-cell number by 24.58% ± 7.98% ($p < 0.004$). At 1 μg/ml heparin, A5-heparin reduced cell numbers by 73.14% ± 2.75%. The amount of polymer used in the conjugate was the highest amount of polymer alone that did not have a significant effect.

### Internalized Heparin Affects Cell Processes

To determine if the conjugate-mediated effects were due to nonspecific cytotoxicity, we examined whether specific cell processes were affected. The effects of internalized heparin on six transcription factor levels in B16-F10 cells were determined. We found a general alteration of specific transcription factors in both the nucleus and the cytoplasm (Figures 3A and 3B). The most striking effect was seen in DP-1 in the nucleus and the cytoplasm, where levels were elevated 2.18- ± 0.12-fold and 2.72- ± 0.03-fold, respectively. Nuclear E2F-1 and Sp-1 were both initially lower than the control but then corrected toward the control. Nuclear p107, Rb, and E2F-2 all showed initial increases compared to the control but subsequently declined. After 4 hr, Rb decreased substantially below the control level. Cytoplasmic p107 and E2F-2 were initially elevated but then returned to near baseline levels. Levels of E2F-1, Rb, and Sp-1 were substantially elevated over time, although Rb did show a relative decrease between 1 hr and 4 hr. The measured levels for the six transcription factors showed an average elevation of 1.20- and 1.63-fold in the nucleus and cytoplasm, respectively, after 4 hr. Without DP-1, the increases were 1.01-fold for nuclear transcription factors and 1.41-fold for cytoplasmic transcription factors.

To examine the occurrence of individual heparan sulfate (HS) epitopes within the HSGAGs present on and around B16-F10 cells, we used a panel of 10 anti-HS antibodies for immunocytological staining of fixed cell cultures. Most antibodies showed strong staining for HS on the cell surface and in the ECM. Antibodies HS4C3 and RB4CD12 showed differential staining patterns between A5-heparin and heparin alone (Figure 3C).

### Growth-Inhibitory Effects Are GAG Specific

To investigate whether the growth-inhibitory effect was specific to heparin or generalized to GAGs of various

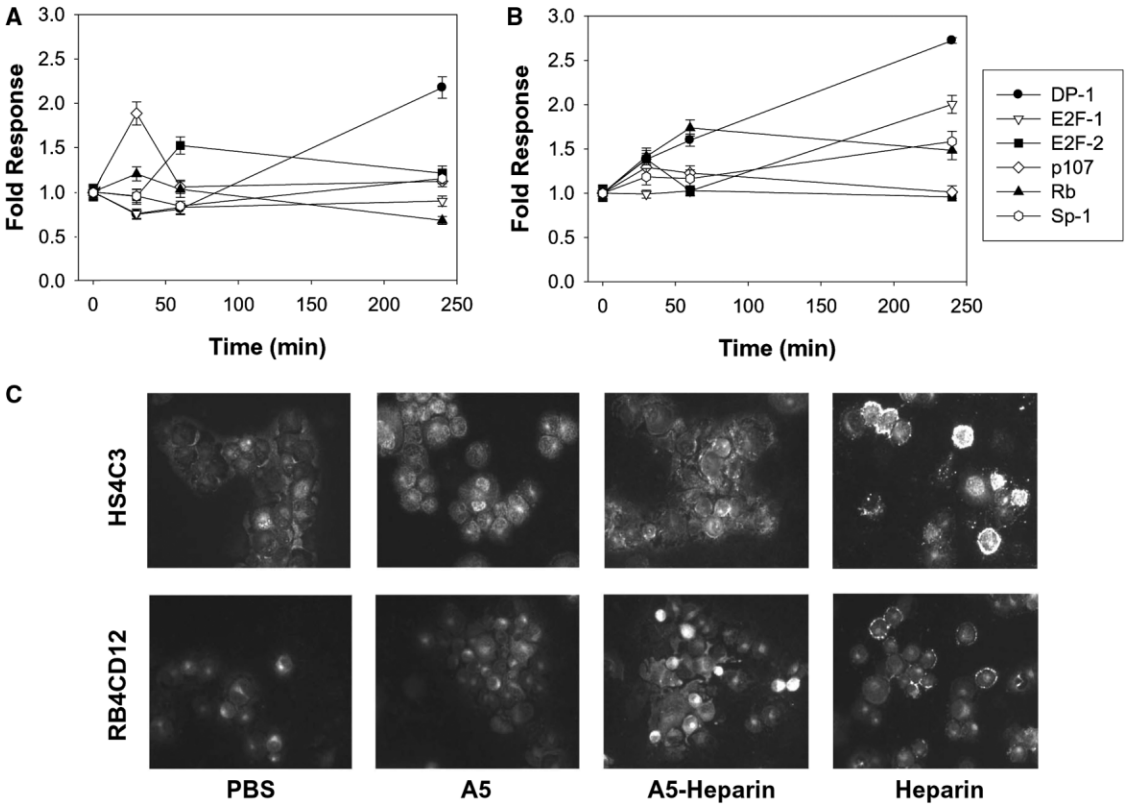


Figure 3. A5-Heparin Affects Cellular Processes

B16-F10 cells were treated with A5-heparin conjugates at a 20:1 (w/w) ratio. (A) Nuclear and (B) cytosolic transcription factor levels were determined after incubation with conjugates for different time periods. Data are normalized to untreated cells with results presented as the relative increase in magnitude compared to untreated cells. (C) Immunohistochemistry of B16-F10 cells after treatment with PBS, A5, A5-heparin conjugates, or heparin with antibodies specific to HS moieties.

size, charge, and composition, heparan sulfate (HS), enoxaparin, low molecular-weight heparin (LMWH) of two activity levels, and two forms of chondroitin sulfate (CS) were tested for their ability to bind A5 and to produce a biological effect in B16-F10 cells via proliferation assays. The composition of the HSGAGs was determined by capillary electrophoresis-based compositional analysis as described [16, 17]. Heparin, enoxaparin, and high-activity LMWH had the highest quantities of sulfate groups, averaging 2.32, 2.41, and 2.35 sulfates per disaccharide, respectively (Figure 4A). HS had only 0.43 sulfates per disaccharide. CS-A was primarily 4-O sulfated, with the corresponding peak constituting 98.2% of total peak area. CS-C was primarily 6-O sulfated but contained some 4-O sulfated disaccharides, as well as three forms of disulfated disaccharides. This collection of GAGs, therefore, allowed for the examination of sulfation degree, length, and saccharide type.

The azure A binding assay demonstrated that A5 bound to all of the GAGs employed at a 20:1 (w/w) A5:heparin ratio in 25 mM sodium acetate. The minimum amount of polymer required for complete binding was higher for GAG species with more sulfates per disaccharide. Correspondingly, A5 (as well as other polymers) bound full-length heparin and highly-sulfated LMWHs with similar efficiency. Heparin induced the greatest reduction in the B16-F10 cell number ($p < 5 \times 10^{-5}$; Figure 4B) of the A5-GAG conjugates (20:1, w/w; 500 ng/ml GAG). The undersulfated HS produced only a 19.70% $\pm$ 4.01% reduction compared to that of 53.73% $\pm$ 5.80% for heparin. The shorter chain enoxaparin and LMWHs also produced reductions in cell number that were lower in magnitude than full-length heparin. It is noteworthy that, compared to other polymers that enabled conjugate internalization, A5 also promoted the maximal cell-mediated effect for LMWHs. Each of the two species of CS had less of an effect than heparin. The 33.12% $\pm$ 5.51% reduction induced by CS-C is significantly greater than the 15.28% $\pm$ 4.52% reduction induced by CS-A ($p < 0.0002$) and the reduction induced by HS ($p < 0.001$).

## Internalized Heparin Promotes a Cell-Specific Response

We examined if A5-heparin affected other cell types. The proliferative effects of A5-heparin (20:1, w/w; 1 $\mu$g/ml heparin) were examined in SMCs, BAECs, FGFR1c-transfected BaF3 cells, SW-1088, SK-ES-1, Panc-1, SK-ES-1, and B16-BL6 by whole-cell proliferation. The A5-heparin conjugate had a minimal effect on SMCs (3.84% $\pm$ 3.33%), BAECs ($-$1.09% $\pm$ 1.94%), transfected BaF3 cells (14.52% $\pm$ 4.05%), B16-BL6 cells ($-$8.92% $\pm$ 12.36%), and Panc-1 cells ($-$2.74% $\pm$ 5.41%), but it did elicit a significant reduction in the

A

| Disaccharide | Heparin | HS | Enoxparin | High Activity LMWH | Low Activity LMWH |
|---|---|---|---|---|---|
| $U_{2S}H_{NS,6S}$ | 58.13 | 1.05 | 63.00 | 57.97 | 0.31 |
| $U_{2S}H_{NS}$ | 5.84 | 0.73 | 3.95 | 4.19 | 60.25 |
| $UH_{NS,6S}$ | 13.74 | 2.13 | 14.82 | 17.04 | 31.50 |
| $U_{2S}H_{NAc,6S}$ | 1.97 | 0.48 | 1.47 | 1.63 | 10.27 |
| $UH_{NS}$ | 4.09 | 15.01 | 2.75 | 3.51 | 0.97 |
| $U_{2S}H_{NAc}$ | 0.90 | 0.26 | 0.67 | 0.20 | 0.12 |
| $UH_{NAc,6S}$ | 9.31 | 18.19 | 7.87 | 11.46 | 0.65 |
| $UH_{NAc}$ | 3.86 | 61.66 | 2.70 | 0.79 | 2.09 |

B

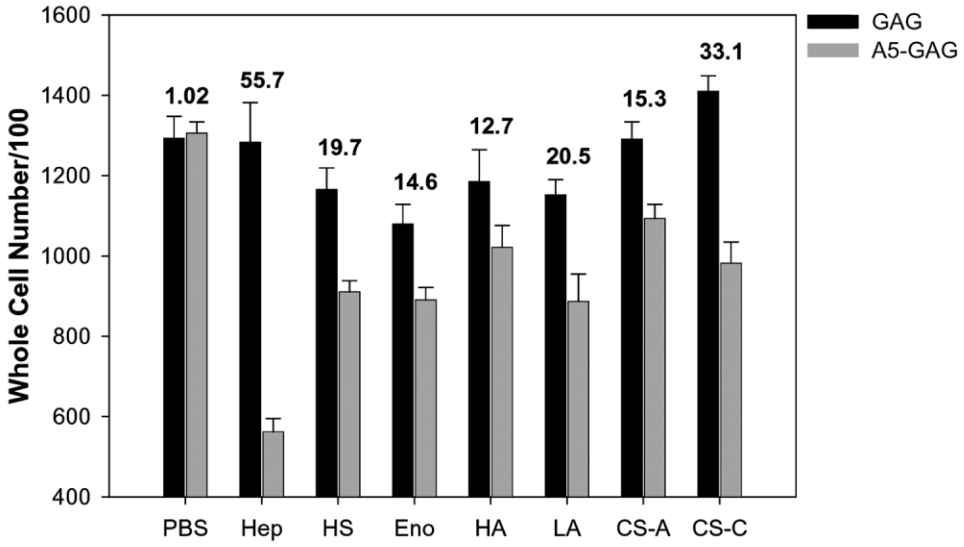


Figure 4. Heparin Induces Greater Growth Inhibition Than Other GAGs

(A) The disaccharide composition of the various pools was determined by capillary electrophoresis after complete digestion by heparinases. Numbers represent the percentage of each given disaccharide. Not included is the undigestable 4-7 tetrasaccharide, which represents the deviation of the sum of each column from 100.

(B) B16-F10 cells were treated with GAGs (black bars) and A5:GAG conjugates (gray bars; 20:1, w/w). Hep, Eno, HA, LA, CS-A, and CS-C refer to heparin, enoxaparin, high-activity LMWH, low-activity LMWH, CS A, and CS C. Data are expressed as a whole-cell number/100. Numbers represent the percent change in the whole-cell number for the A5:GAG conjugate compared to GAG alone.

whole-cell number of SK-ES-1 (53.79% ± 7.85%) and SW-1088 (23.76% ± 8.89%) cells. Proliferation assays were also performed in the presence of each of 10% fetal bovine serum (FBS), 50 mM sodium chlorate, and 5 ng/ml FGF2 (50 ng/ml for transfected BaF3 cells). The presence of FBS significantly reduced the effect of the conjugate. Sodium chlorate, which abrogates cell surface HSPGs [7], reduced the growth-inhibitory effects of A5-heparin in SK-ES-1 and SW-1088 cells (Figure 5A). The effect of A5-heparin in the presence of FGF2 was not significantly different from the summed changes induced separately by conjugate and FGF2.

The cell-specific effects of A5-heparin raised the question as to why certain cells were more affected. The results could not be directly attributed to cell turnover rate because transfected BaF3 cells and SMCs, which are not susceptible to A5-heparin conjugate-mediated reductions, have a faster turnover rate than SW-1088 cells, which are susceptible. Given that the polymer likely enables internalization by promoting endocytosis [10], we investigated whether internalization rates could be the source of the differential effects observed. Fluorescein-conjugated heparin was used for measuring internalization rates in SMCs, B16-BL6 cells, and B16-F10 cells. B16-F10 cells show internalization of heparin within 1 hr (Figure 5B). Neither SMCs nor B16-BL6 cells showed significant internalization within 6 hr, although all three cell lines demonstrated internalized conjugate after 24 hr. These results confirm the cell-specific nature of A5-heparin conjugate-mediated inhibition of proliferation and suggest that selectivity is related to the complexes' rate of uptake.

### Internalized Heparin Induces Cell Death

We next sought to determine whether internalization of heparin by A5 affects specific cell processes and thus reduces the whole-cell number. We used $^{3}$H-thymidine incorporation to measure DNA synthesis in B16-F10 cells after the application of A5-heparin. The mitogenic response followed a dose-response curve, wherein low concentrations of A5-heparin *promote* $^{3}$H-thymidine incorporation and high doses inhibit it (Figure 6A). None

A

| A5-Heparin | B16-F10 | SK-ES-1 | SW-1088 | BaF3 |
|---|---|---|---|---|
| Unsupplemented | 58.28 ± 12.97 | 53.79 ± 7.85 | 23.76 ± 8.89 | 14.59 ± 4.05 |
| FGF2 | 86.51 ± 1.05 | 48.12 ± 12.21 | 21.67 ± 11.47 | 14.52 ± 10.70 |
| Chlorate | 54.39 ± 11.06 | 31.71 ± 19.18 | 3.36 ± 6.00 | N/A |

B

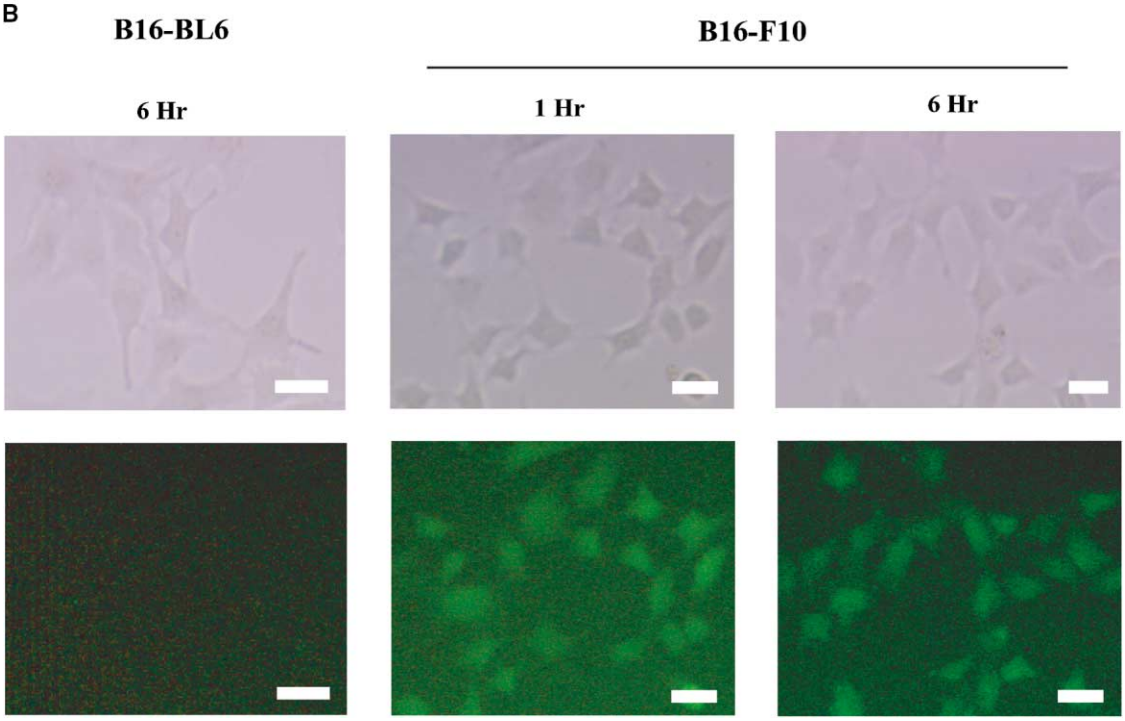


Figure 5. A5-Heparin Exhibits Cell Selectivity

(A) Cells were treated with A5-heparin (20:1, w/w; 1 μg/ml heparin) supplemented with PBS, FGF2, or sodium chlorate. Data are presented as a percent of the whole-cell count compared to the count for treatment without A5-heparin. Transfected BaF3 cells were not examined in the presence of chlorate as a result of the lack of cell surface GAGs.

(B) B16-BL6 and B16-F10 cells were treated with A5-fluorescein-labeled heparin conjugates (20:1, w/w; 1 μg/ml). Cells were imaged with light microscopy, and fluorescein was visualized with fluorescence microscopy. Scale bars represent 10 μm.

of the equivalent A5 concentrations (20-fold greater than the heparin concentration), including the highest concentration tested, 100 μg/ml, elicited a change in mitogenesis.

The mechanism by which A5-heparin conjugates induced their effects was also examined with a lactic-acid dehydrogenase (LDH) cytotoxicity assay and a caspase-3/-7 apoptosis assay. Heparin, A5, and A5-heparin all significantly increased LDH detection compared to that in the untreated condition (Figure 6B). Heparin, A5, and A5-heparin elicited responses that were 50.70% ± 13.81%, 35.69% ± 18.94%, and 77.93% ± 11.91%, respectively, of that caused by Triton-X, the positive control. A5-heparin conjugate activated caspase-3/-7 levels to an extent comparable to that of camptothecin, the positive control (Figure 6C). Compared to PBS, neither heparin nor A5 alone promoted a significant elevation of caspase activity, thereby suggesting that the conjugation of A5 and heparin promoted apoptosis in a way unobserved with either component alone.

### A5-Heparin Promotes Early Spermine Incorporation

Spermine incorporation was investigated not only because cell surface HS binds to the spermine transporter, which promotes the uptake of spermine, but also because cellular proliferation is dependent on an adequate supply of polyamines [18, 19]. To this end, $^{14}$C-spermine incorporation was measured over time subsequent to A5-heparin administration in SMCs and B16-BL6 and B16-F10 cells. SMCs and B16-BL6 cells showed a significant influx of $^{14}$C-spermine at the 6 hr time point (Figure 7). The magnitude of this effect was 43.97% and 41.83% of that induced by difluoromethylornithine (DFMO) in SMCs and B16-BL6 cells, respectively. However, we observed an influx of $^{14}$C-spermine that was 19.61-fold greater than that observed with DFMO at 6 hr in B16-F10 cells. Furthermore, at the 9 hr time point, B16-F10 cells had 2-fold greater incorporation.

## Discussion

### Cationic Polymers Can Bind and Internalize Heparin

The internalization of HSGAGs into cells has been seen as an event involved with specific processes, including growth factor signaling and membrane transcytosis. HSGAGs bind to FGF2 and FGFR1 to form a ternary complex that is internalized by endocytosis [7, 8].

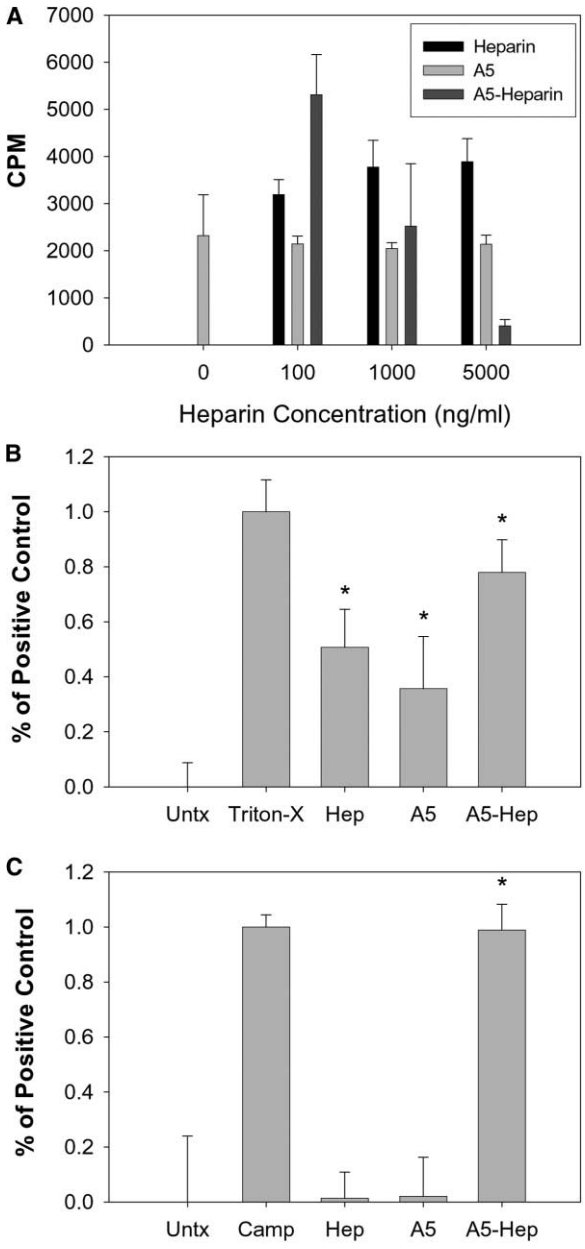


Figure 6. A5-Heparin Induces Cell Death

B16-F10 cells were treated with A5-heparin conjugates at a 20:1 (w/w) ratio or with equivalent concentrations of A5 or heparin alone. (A) $^{3}$H-thymidine incorporation was measured as CPM over a range of heparin concentrations. A concentration of 0 ng/ml represents untreated cells. (B) Cytotoxicity measured by an LDH assay was determined at 1 $\mu$g/ml heparin. Untx and Hep represent untreated and heparin cells, respectively. Data are presented as the percent of the positive control, determined as follows: (experimental point − negative control)/(positive control – negative control), where untreated is the negative control and Triton-X is the positive control. (C) Apoptotic activity measured by caspase-3/-7 assays was determined at a heparin concentration of 1 $\mu$g/ml. Untx, Camp, and Hep represent untreated, camptothecin, and heparin, respectively. Data are presented as the percent of the positive control, where untreated is the negative control and camptothecin is the positive control. An asterisk denotes $p < 0.05$ compared to the negative control.

HSGAGs can also facilitate membrane transcytosis, such as at the blood-brain barrier [20]. The function of HSGAGs in these cases is to regulate the biological response to and the localization of growth factors. The specific internalization of heparin as a model HSGAG could therefore, theoretically, be used for modulating cell processes involving HSGAGs within the confines of the cell.

Herein, we utilized PAEs, a class of polymers that interact with DNA via a charge-mediated mechanism. PAEs are an ideal class of polymers for delivery of DNA as a result of their low toxicity compared to that of other polymeric methods of DNA delivery, their rapid biodegradability into biologically inert compounds, and their simple synthesis [10, 11]. The primary anionic region of heparin is in the sulfate groups at the N-, 2-O, 3-O, and 6-O positions on the disaccharides that compose heparin. The high quantity of sulfate groups on heparin confers a greater negative charge than DNA [21]. Because of this, of the 70 water-soluble PAEs from a screening library of 140, all bound heparin at a 20:1 w/w ratio in optimal conditions (25 mM sodium acetate [pH 5.0]). Substantial binding is similarly facilitated at suboptimal conditions. However, only a small subset of these polymers enable internalization of heparin into cells. The fact that PAEs do not enable heparin internalization as well as DNA is not surprising, however, given that a net positive charge, which may trigger endocytosis by promoting interactions with the negatively charged cell membrane, would be more difficult to achieve with a more anionic biopolymer [13]. Correspondingly, the PAEs that mediated the highest levels of DNA internalization had the most positive zeta potentials [15]. The fact that PAEs do not enable heparin internalization as well as DNA is consistent with a net positive charge required for endocytosis. Although lysosomal escape was not specifically examined here, cationic surfaces promote interactions with the lysosome membrane and subsequent release into the cytosol [22]. Therefore, the positive zeta potentials are consistent with lysosomal escape. Apoptotic bodies visible in cultures after the addition of fluorescein-heparin conjugated to polymers uniformly exhibited fluorescence (Figure 1), suggesting even distribution of the conjugates throughout the cytosol. Furthermore, we surmise that the A5-heparin conjugate must escape into the cytosol to significantly alter the activities of transcription factors and caspaces.

### Internalized Heparin Affects Cell Processes

The 14 PAEs that internalized heparin had distinct response levels when examined in a whole-cell proliferation assay. Polymer A5 was used because the magnitude of change in the whole-cell number was greatest, suggesting either the presence of the highest quantity of internalized heparin or the most robust response induced by the internalized complex. The ability of A5-heparin conjugates as opposed to heparin or A5 alone, to affect the whole-cell number, transcription factor levels, and the HSGAG epitopes present on and around the cell, is consistent with internalization of the complex. Furthermore, complexes formed with PAEs that were shown by assays performed herein to bind but not internalize heparin had no effect on the whole-cell number.

The cellular response to A5-heparin was found to be cell specific (Figure 5A). In general, noncancerous cells

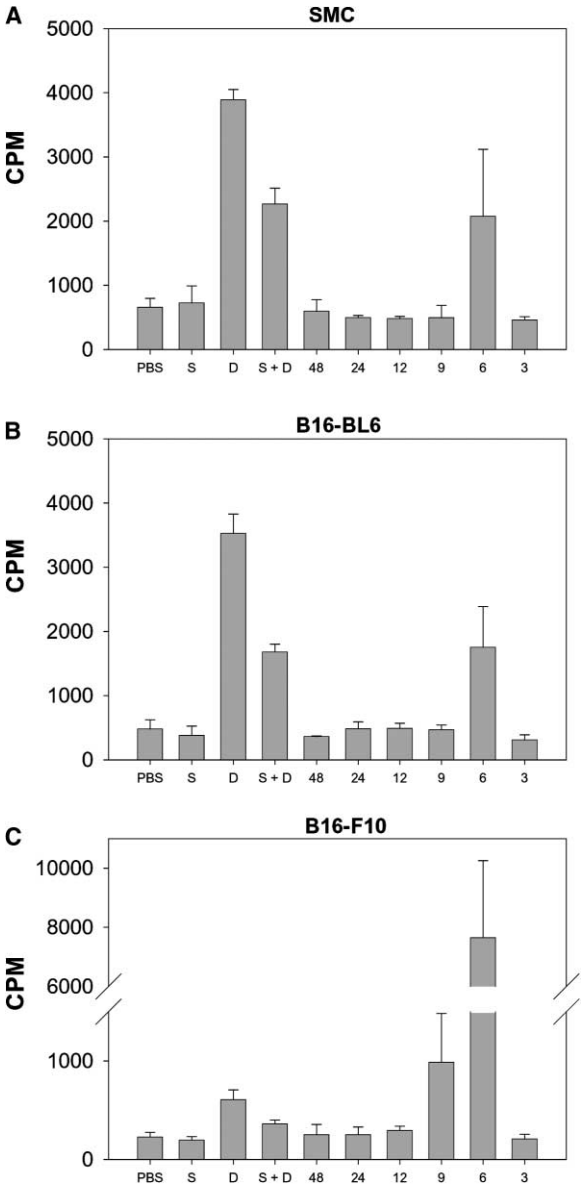


Figure 7. A5-Heparin Induces Spermine Incorporation at 6 hr

Incorporation of $^{14}$C-spermine was measured over time after treatment of (A) SMCs, (B) B16-BL6 cells, and (C) B16-F10 with A5:heparin conjugates (20:1, w/w; 1 μg/ml). S and D denote 5 μM spermine and 5 mM DFMO, respectively. Numbers along the *x*-axis reflect conjugate incubation time. Data are presented as CPM.

produced a lower magnitude of effect than cancer cells. The upregulation of huntingtin-interacting protein-1, a cofactor in clatharin-mediated endocytosis, has been associated with various epithelial cancers [23, 24]. Endocytic rate has been demonstrated to govern cell sensitivity to exogenous agents [25]. Correspondingly, B16-F10 cells, which exhibited the greatest magnitude of response to A5-heparin conjugates, showed a much faster rate of conjugate internalization than other cells, in which less pronounced responses were induced (Figure 5B). Spermine incorporation, which is greatly increased in susceptible cells, showed maximal effects after 6 hr. SMCs and B16-BL6 cells did not show significant internalization at this time and, correspondingly, elicited lower levels of spermine incorporation (Figure 7). B16-F10s, which internalized A5-heparin conjugates within 1 hr, showed much greater levels of spermine incorporation. Cell selectivity therefore seems dependent on internalization rate.

### Full-Length Heparin Promotes the Greatest Biological Response

The biological effect of internalized GAGs is not limited to heparin. Compared to GAG or polymer A5 alone, heparin, HS, LMWHs, and CS each induced some reduction in the whole-cell number. Full-length heparin, however, induced the largest effect. Heparin has the highest charge density of the four full-length GAGs tested. High-activity LMWH, however, has a similar charge density to, but a smaller biological effect than, full-length heparin. Although the relative amount of each internalized GAG was not quantified, these results suggest that high molecular weights and higher charge densities confer greater activity. Correspondingly, partial digestion of heparin with heparinase I (hepI) [17], which cleaves highly sulfated regions of HSGAGs prior to conjugation with polymer A5, reduces the magnitude of effect observed. Although hepIII digestion, which targets undersulfated regions, also reduces the magnitude of response, the reduction is less than that observed with hepI treatment (data not shown).

### Internalized Heparin Induces Apoptosis

Reduction of the whole-cell number does not directly explain the mechanism of action or distinguish between general toxicity and controlled alterations to cell processes. We therefore sought to probe how internalized heparin induced cellular effects. We hypothesized that internalized heparin induces cell-mediated responses by affecting cell processes normally involving heparin, altering cell functions by the degree of negative charge in the cell, or preventing transcription factor binding.

FGF2 has an essential autocrine role in melanoma [26]. Furthermore, the FGF-FGFR complex is stabilized, and heparin promotes downstream signaling [27, 28]. The FGF2 system therefore provides an ideal approach for examining if internalized heparin alters cell processes normally involving heparin. The effects of A5-heparin conjugates in the presence of FGF2 did not yield a reduction in the whole-cell number that was distinct from the sum of the independent effects of the conjugates and FGF2. The affect of conjugates in the presence of FGF2 was similarly additive in all cell lines examined. Furthermore, when normalized to the affects of FGF2 alone the affects of internalized heparin are identical on BaF3 cells as well as those transfected with FGFR1 (data not shown). Taken together, these results suggest internalized heparin does not directly affect FGF2 signaling.

The Rb pathway is another critical pathway in the development of melanoma [29]. The mutation of Rb and other tumor suppressor proteins, including p107, causes an increase in the number of free E2F family members present [30]. We found that internalized hepa-

rin led to an upregulation of nuclear E2F-2 and cytoplasmic E2F-1. Furthermore, Rb was upregulated in the cytoplasm but downregulated in the nucleus. The levels of p107 were generally unchanged. DP-1 is not typically associated with melanomas but has been found to be upregulated in complexes with E2F [31]. Sp-1, which is similarly not thought of as important in melanomas, was upregulated in tumors, including glioblastomas [32]. With the exception of elevated levels of Rb found in the cytoplasm, the internalization of heparin promotes a cellular response that is in accordance with *promoting* melanoma growth.

Heparin internalization places a substantial quantity of a highly charged compound into cells. Although this could adversely affect cells by a nonspecific process, controlled internalization of 0.15 M trehalose actually *protects* cells from environmental changes [33]. With the addition of 1 $\mu$g heparin to $5 \times 10^4$ cells, each cell could receive up to 20 pg of internalized heparin, or $\sim$.13 M heparin, suggesting that a purely osmotic effect is unlikely. Furthermore, HA-LMWH, which has the same charge density as full-length heparin, has a much lower capacity to reduce the whole-cell number. Therefore, nonspecific charge-mediated effects do not appear to be the source of the observed biological response.

Oligosaccharides have previously been demonstrated to bind transcription factors [34]. Additionally, heparin is used for assessing the binding strength of delivery systems to DNA because the greater charge density of heparin can compete with and force charged molecules off of DNA. We found a generalized upregulation of transcription factors in both the cytosol and the nucleus. Because an ELISA technique was used for quantifying transcription factor levels, heparin could apparently increase transcription factor levels by competing with and forcing transcription factors off of DNA and thereby freeing the binding sites. Antithrombin III, however, prevents NF-$\kappa$B activation and the subsequent production of growth factors and cytokines in a heparin-dependent manner [35]. Internalized heparin therefore likely inhibits transcription factor activity either by preferentially binding DNA or by inhibiting transcription factor activation. The alterations in mitogenic response and caspase-3/-7 activity (Figure 6) are consistent with specific cell processes being affected to induce apoptosis. These results suggest that internalized heparin reduces cell numbers by inducing apoptotic cell death via a transcription factor-mediated mechanism.

This report details a novel mechanism by which large, highly charged polysaccharides can be delivered into cells. This delivery induces a cell-specific apoptotic response, based primarily on the rate at which complexes are internalized. Because certain cancers have a higher endocytic rate, the use of internalized heparin may offer a novel approach for treating cancers. Additionally, because heparin can bind several growth factors and cytokines, delivery of heparin could serve as a platform for the development of combination therapies to treat cancer. Further work is still necessary to elucidate the specific mechanism by which internalized heparin induces apoptosis as well as to elucidate its efficacy in other cancers.

## Significance

**Heparin/heparan sulfate-like glycosaminoglycans (HSGAGs) are anionic biopolymers involved in diverse cellular processes in the extracellular matrix. Heparin is a prototypical HSGAG that is more negatively charged than other HSGAGs as a result of the high quantity of sulfate groups found on the composite disaccharides. A library of polymers, poly(β-amino ester)s, which interact with DNA via a charge-mediated mechanism and enable its internalization, were used for investigating the impact of free heparin within the cell. HSGAGs are normally internalized but are protein bound in the process. All water-soluble polymers bound heparin but only 14 allowed for heparin internalization. Of importance, cationic polymers that sufficiently bind heparin can promote its uptake into cells. Fewer poly(β-amino ester)s enabled internalization of heparin than of DNA, which is consistent with conjugate endocytosis requiring a net positive charge. Only a subset of polymers that can internalize DNA would be sufficiently cationic to internalize the more anionic heparin. Polymers developed for intracellular delivery of anionic compounds therefore need a sufficient positive charge to compensate for the molecule delivered. Furthermore, the uptake of heparin into the cell induces apoptotic cell death that is preferential to specific cell types because of internalization rates. Cancer cells, which have a faster endocytic rate than noncancerous cells and correspondingly take up polymer-heparin conjugate more quickly, are typically more susceptible to the effects of polymer-heparin conjugates. Although targeting cancer based on endocytic rate alone would likely affect macrophages and neutrophils as well, local delivery could allow for induction of cancer cell death with minimal effects to surrounding tissues. Therefore, internalizing heparin with poly(β-amino ester)s offers a new approach to induce cancer cell death.**

## Experimental Procedures

### Proteins and Reagents

Porcine intestinal mucosa heparin was from Celsus Laboratories (Columbus, OH). FBS was from Hyclone (Logan, UT). Minimal essential medium (MEM), Dulbecco's modified Eagle medium (DMEM), RPMI-1640, L-15, phosphate buffered saline (PBS), L-glutamine, and penicillin/streptomycin were obtained from GibcoBRL (Gaithersberg, MD). Mouse recombinant IL-3 was from R & D Systems (Minneapolis, MN). B16-BL6, B16-F10, Panc-1, SK-ES-1, and SW-1088 cells were from the American Type Culture Collection (Manassas, VA). Dithiothretol (DTT) and the protease inhibitor cocktail were from Sigma (St. Louis, MO). BaF3 cells transfected with FGFR1c [16] were generously provided by Dr. David Ornitz (Washington University, St. Louis, MO). NIH 3T3 cells were generously provided by Dr. Matthew Nugent (Boston University School of Medicine, Boston, MA).

### Polymer-Heparin Conjugate Synthesis

Polymers were prepared and conjugated to heparin via a similar method as that described for DNA [11]. Each polymer is named by its composite diacrylate (A–F) and amine (1–20). In brief, polymers were dissolved via vortexing in 25 mM sodium acetate (pH 5.0) and then mixed with heparin in 25 mM sodium acetate( pH 5.0) to produce the desired polymer:heparin ratio (w/w). The mixture was

shaken for 30 min at room temperature. Complexes were stored at 4°C until use, which was no greater than 3 hr after conjugation.

### Azure A Heparin Binding Assay

The individual effects of heparin and polymer on the azure A colorimetric assay were first established. Azure A was dissolved in sodium acetate (pH 5.0) to produce a 0.2% (w/v) solution. Heparin and each of the 70 library-derived polymers that are soluble in sodium acetate (pH 5.0) [11] were dissolved in it to produce solutions ranging between 10 ng/ml and 1 mg/ml. Each sample at each concentration was mixed thoroughly at a 1:1 ratio with azure A in a final volume of 1 ml, and the absorbance was determined at 596 nm [36].

For polymer-azure A competition assays, 250 μl of 20 μg/ml heparin in 25 mM sodium acetate (pH 5.0) was mixed with 250 μl of each of the 70 polymers in 25 mM sodium acetate to yield a final polymer:heparin ratio (w/w) of 1:1, 5:1, 10:1, or 20:1. Each 500 μl solution was shaken for 30 min at room temperature to allow for conjugation and then supplemented with 500 μl azure A solution. The resultant solution was incubated for 5 min at room temperature and mixed thoroughly, and the absorbance was measured at 596 nm. The amount of free heparin capable of binding azure A after polymer:heparin complexes were produced was determined by comparison of the resulting $A_{596}$ to a standard heparin curve.

### Cell Culture

SMCs were isolated as described [37]. SMCs, BAECs, NIH 3T3 mouse fibroblast cells, and Panc-1 human pancreatic adenocarcinoma cells were maintained in DMEM supplemented with 10% FBS. B16-BL6 and B16-F10 mouse melanoma cells were maintained in αMEM supplemented with 10% FBS. SK-ES-1 human anablastic osteosarcoma cells were maintained in 5a media supplemented with 15% FBS. SW-1088 human astrocytoma cells were maintained in L-15 media supplemented with 10% FBS. All media were supplemented with 100 μg/ml penicillin, 100 U/ml streptomycin, and 500 μg/ml L-glutamine. Adhesion cells were grown in 75 $cm^2$ flasks or 150 $cm^2$ dishes at 37°C in a 5% $CO_2$ humidified incubator and passaged 2–3 times per week at confluence.

FGFR1c-transfected BaF3 cells were maintained as suspension cultures in RPMI-1640 supplemented with 10% FBS and 500 ng mouse recombinant IL-3. Cultures were grown in 75 $cm^2$ flasks at 37°C in a 5% $CO_2$ humidified incubator and passaged at a 1:10 dilution three times a week.

### Conjugate Internalization

Fluorescein-conjugated heparin (Molecular Probes, Eugene, OR) was complexed with polymers as for unconjugated heparin. BAECs, SMCs, and NIH 3T3 cells were grown until confluent, washed with PBS, treated with 4 ml trypsin-EDTA per 150 $cm^2$ tissue culture dish at 37°C for 3–5 min, and collected with 10 ml media. The suspension was pelleted and resuspended in 10 ml proliferation media. Cell concentration was determined with an electronic cell counter, and the solution was diluted to $5 \times 10^4$ cells/ml. Wells of 96-well plates were supplemented with 100 μl of cell suspension. For each cell type, three wells per polymer were treated with polymer-heparin conjugates at a 20:1 (w/w) ratio to yield a final heparin concentration of 500 ng/ml. Three wells were treated with an equivalent amount of polymer alone. Three wells for each cell type were treated with fluorescein-labeled heparin. Three wells per cell type contained untreated cells. The plates were incubated for 24 hr at 37°C and 5% $CO_2$ and visualized with fluorescence microscopy. Conjugates were defined as having enabled heparin internalization if 80% of cells showed fluorescence colocalized with cells in 7 of 10 high-powered fields in each of the three wells for the given conjugate, and less than 20% of cells treated with labeled heparin alone in 7 of 10 high-powered fields for each of the three wells showed similar colocalization of fluorescence with cells.

For evaluation of internalization rates, SMCs, B16-BL6 cells, and B16-F10 cells were seeded at $5 \times 10^4$ cells/ml in 24-well plates. Three wells for each cell type were treated with 10 μl PBS, A5-fluorescein-labeled heparin conjugates (20:1, w/w; 1 μg/ml), fluorescein-labeled heparin (1 μg/ml), or uncomplexed A5 alone (20 μg/ml). Cells were visualized with fluorescence microscopy every hour for 6 hr and again after 24 hr. Requirements for defining internalization were as described. Digital images were processed with Adobe Illustrator 10.0 and Adobe Photoshop 7.0.

### Whole-Cell Proliferation Assay

Adhesion cells (B16-F10, B16-BL6, SMCs, BAECs, NIH 3T3, SK-ES-1, Panc-1, and SW-1088) were seeded in 24-well plates at 1 ml/well as well as in 6-well plates at 3 ml/well, both at a density of $5 \times 10^4$ cells/ml. The plates were incubated for 24 hr at 37°C and 5% $CO_2$. The cells were then washed with PBS and supplemented with media as appropriate. Cells were treated with PBS, heparin, polymer, or polymer-heparin conjugate in 10 μl quantities at appropriate concentrations. Cells were incubated at 37°C and 5% $CO_2$ for 72 hr. Subsequently, each well was treated with 500 μl (24-well plates) or 1 ml (6-well plates) trypsin-EDTA for 5–15 min at room temperature, and 400 μl was used for counting the cell number with an electronic cell counter. Assays were performed in the presence of 0.1% FBS supplemented with PBS, 5 ng/ml FGF2, or 50 mM sodium chlorate. Panc-1 cells were only tested in 10% FBS. The effects of conjugates were normalized to that of cotreatment without conjugates.

Proliferation assays on transfected BaF3 cells were performed as described [39] with slight modification. Cells were collected from 75 $cm^2$ flasks, washed three times with FBS-deficient media, and resuspended in 10 ml FBS-deficient media. Cells were diluted to $1 \times 10^5$ cells/ml based on the reading of an electronic cell counter and plated 1 ml/well in 24-well plates. Wells were treated with PBS, heparin, polymer, or polymer:heparin conjugate in 10 μl volumes and incubated for 72 hr at 37°C and 5% $CO_2$. Cell counts were determined with an electronic cell counter. The conditions employed were similar to those used for adherent cells except that FGF2 was applied at a concentration of 50 ng/ml [38]. The effects of the conjugate were normalized to the no-conjugate condition.

### Immunohistochemistry

B16-F10 cultures were washed three times with PBS, dried overnight, and stored at −80°C until use. Cell cultures were rehydrated in PBS for 10 min. After being blocked for 20 min in PBS containing 0.1% (w/v) BSA, cultures were incubated with c-Myc-tagged and VSV-tagged anti-HS antibodies (AO4B05, AO4B08, AO4F12, HS4A5, HS4C3, RB4CD12, RB4CB9, RB4EA12, EW4A11, and EW4G2) overnight [39, 40]. Bound antibodies were visualized with either an anti-c-Myc-chicken monoclonal antibody (A21281; Molecular Probes) for 90 min and then an Alexa 594-conjugated goat anti-chicken IgG antibody for 60 min (A11042; Molecular Probes), or a Cy-3-labeled anti-VSV monoclonal antibody (9E10; Sigma). Cultures were washed three times for 10 min (each time) with PBS after each incubation. Finally, cultures were fixed in 100% methanol, dried, and embedded in Mowiol (10% [w/v] in 0.1 M Tris-HCl [pH 8.5]/25% [v/v] glycerol/2.5% [w/v] $NaN_3$). As a control, primary, secondary, or conjugated antibodies were omitted. All incubations were performed at ambient temperature (21°C) with antibody titers of half the dilution factor at which signal was abolished. Photographs were taken with a constant aperture and shutter time on a Zeiss Axioskop immunofluorescence microscope (Göttingen, Germany) equipped with a Kodak KAF 1400 CCD. Digital images were processed with Adobe Photoshop 7.0.

### Mitogenic Assay

B16-F10 cells were plated in 24-well plates at $5 \times 10^4$ cells/ml in 1 ml/well. Cells were serum starved for 24 hr. Polymer-GAG conjugates were added in 10 μl volumes and incubated for 20 hr. Cells were incubated with 1 μCi/ml $^3$H-thymidine (Perkin Elmer, Wellesley, MA) for 4 hr, washed with PBS, and treated with 500 μl of 1 M NaOH per well. The contents of each well were transferred to 7 ml scintillation vials containing 5 ml scintillation fluid and counted with a scintillation counter. Data are reported as counts per minute (CPM).

### Transcription Factor and Cell Death Assays

For assessing the affects on transcription factors, B16-F10 cells were seeded at $5 \times 10^4$ cells/ml in 6-well plates in propagation media. Cells were serum starved and subsequently treated with PBS, A5 (20 μg/ml), heparin (μg/ml), or A5-heparin formulated at a 20:1 ratio (w/w). ELISA for transcription factors DP-1, E2F-1, E2F-2, p107, Rb, and Sp-1 proceeded according to the manufacturer's

protocol (BD Biosciences, Palo Alto, CA). The relative change in transcription factor levels was measured with a spectrophotometric plate reader at 655 nm.

The LDH cytotoxicity assay (Roche, Basel, Switzerland) and the Caspase-3/7 apoptosis assay (Roche) were performed according to the manufacturers' instructions. B16-F10, B16-BL6, NIH 3T3, Panc-1, SK-ES-1, and SW-1088 cells were grown to confluence in 150 $cm^2$ dishes. Cells were trypsinized, pelleted, and resuspended in media. Cell concentration was determined with an electronic cell counter. The cell suspension was diluted, and cells were plated in 96-well plates as appropriate. The assays proceeded as described, and the results were determined with a spectrophotometric plate reader.

### Spermine Incorporation Assay

Spermine incorporation was determined as described [19] with slight modification. SMCs, B16-BL6 cells, and B16-F10 cells were seeded at $5 \times 10^4$ cells/ml in 24-well plates in propagation media. Cultures were grown for 24 hr, washed twice with PBS, and supplemented with FBS-deficient media with 5 $\mu$M $^{14}$C-spermine (Amersham Biosciences, Piscataway, NJ). Cells were immediately treated with PBS, heparin (1 $\mu$g/ml), A5 (20 $\mu$g/ml), or A5:heparin (20:1, w/w). Cells were treated with 5 mM DFMO, 5 $\mu$M spermine, or both DFMO and spermine as controls. After 3, 6, 9, 12, 24, and 48 hr incubations, cells were chilled and washed with ice-cold FBS-deficient media containing 1 mM spermine. Cells were lysed with 0.5 ml NaOH, which was then added to 5 ml scintillation fluid, and incorporation was determined with a scintillation counter.

### Acknowledgments

This work was supported by National Institutes of Health grants GM-26698, CA-52857 (R.L.), and HL-59966 (R.S.). D.B. is supported by a Howard Hughes Medical Institute predoctoral fellowship.

Received: November 14, 2003
Revised: January 6, 2004
Accepted: January 9, 2004
Published: April 16, 2004

### References

1. Sasisekharan, R., Shriver, Z., Venkataraman, G., and Narayanasami, U. (2002). Roles of heparan-sulphate glycosaminoglycans in cancer. Nat. Rev. Cancer *2*, 521–528.
2. Perrimon, N., and Bernfield, M. (2000). Specificities of heparan sulphate proteoglycans in developmental processes. Nature *404*, 725–728.
3. Conrad, H.E. (1998). Heparin-Binding Proteins (San Diego: Academic Press).
4. Esko, J.D., and Lindahl, U. (2001). Molecular diversity of heparan sulfate. J. Clin. Invest. *108*, 169–173.
5. Blackhall, F.H., Merry, C.L., Davies, E.J., and Jayson, G.C. (2001). Heparan sulfate proteoglycans and cancer. Br. J. Cancer *85*, 1094–1098.
6. Liu, D., Shriver, Z., Venkataraman, G., El Shabrawi, Y., and Sasisekharan, R. (2002). Tumor cell surface heparan sulfate as cryptic promoters or inhibitors of tumor growth and metastasis. Proc. Natl. Acad. Sci. USA *99*, 568–573.
7. Sperinde, G.V., and Nugent, M.A. (2000). Mechanisms of fibroblast growth factor 2 intracellular processing: a kinetic analysis of the role of heparan sulfate proteoglycans. Biochemistry *39*, 3788–3796.
8. Pellegrini, L., Burke, D.F., von Delft, F., Mulloy, B., and Blundell, T.L. (2000). Crystal structure of fibroblast growth factor receptor ectodomain bound to ligand and heparin. Nature *407*, 1029–1034.
9. Hsia, E., Richardson, T.P., and Nugent, M.A. (2003). Nuclear localization of basic fibroblast growth factor is mediated by heparan sulfate proteoglycans through protein kinase C signaling. J. Cell. Biochem. *88*, 1214–1225.
10. Lynn, D.M., and Langer, R. (2000). Degradable poly(β-amino esters): synthesis, characterization, and self-assembly with plasmid DNA. J. Am. Chem. Soc. *122*, 10761–10768.
11. Lynn, D.M., Anderson, D.G., Putnam, D., and Langer, R. (2001). Accelerated discovery of synthetic transfection vectors: parallel synthesis and screening of a degradable polymer library. J. Am. Chem. Soc. *123*, 8155–8156.
12. Brazeau, G.A., Attia, S., Poxon, S., and Hughes, J.A. (1998). In vitro myotoxicity of selected cationic macromolecules used in non-viral gene delivery. Pharm. Res. *15*, 680–684.
13. Kabanov, A.V., and Kabanov, V.A. (1995). DNA complexes with polycations for the delivery of genetic material into cells. Bioconjug. Chem. *6*, 7–20.
14. Wang, L., Malsch, R., and Harenberg, J. (1997). Heparins, low-molecular-weight heparins, and other glycosaminoglycans analyzed by agarose gel electrophoresis and azure A-silver staining. Semin. Thromb. Hemost. *23*, 11–16.
15. Akinc, A., Lynn, D.M., Anderson, D.G., and Langer, R. (2003). Parallel synthesis and biophysical characterization of a degradable polymer library for gene delivery. J. Am. Chem. Soc. *125*, 5316–5323.
16. Berry, D., Kwan, C.P., Shriver, Z., Venkataraman, G., and Sasisekharan, R. (2001). Distinct heparan sulfate glycosaminoglycans are responsible for mediating fibroblast growth factor-2 biological activity through different fibroblast growth factor receptors. FASEB J. *15*, 1422–1424.
17. Berry, D., Shriver, Z., Natke, B., Kwan, C., Venkataraman, G., and Sasisekharan, R. (2003). Heparan sulfate glycosaminoglycan derived from endothelial cells and smooth muscle cells differentially modulate fibroblast growth factor-2 biological activity through fibroblast growth factor receptor-1. Biochem. J. *373*, 241–249.
18. Belting, M., Havsmark, B., Jonsson, M., Persson, S., and Fransson, L.A. (1996). Heparan sulphate/heparin glycosaminoglycans with strong affinity for the growth-promoter spermine have high antiproliferative activity. Glycobiology *6*, 121–129.
19. Belting, M., Borsig, L., Fuster, M.M., Brown, J.R., Persson, L., Fransson, L.A., and Esko, J.D. (2002). Tumor attenuation by combined heparan sulfate and polyamine depletion. Proc. Natl. Acad. Sci. USA *99*, 371–376.
20. Deguchi, Y., Okutsu, H., Okura, T., Yamada, S., Kimura, R., Yuge, T., Furukawa, A., Morimoto, K., Tachikawa, M., Ohtsuki, S., et al. (2002). Internalization of basic fibroblast growth factor at the mouse blood-brain barrier involves a heparan sulfate proteoglycan. J. Neurochem. *83*, 381–389.
21. Piepkorn, M.W., and Daynes, R.A. (1983). Heparin effect on DNA synthesis in a murine fibrosarcoma cell line: influence of anionic density. J. Natl. Cancer Inst. *71*, 615–618.
22. Panyam, J., Zhou, W.Z., Prabha, S., Sahoo, S.K., and Labhasetwar, V. (2002). Rapid endo-lysosomal escape of poly(DL-lactide-co-glycolide) nanoparticles: implications for drug and gene delivery. FASEB J. *16*, 1217–1226.
23. Ross, T.S., and Gilliland, D.G. (1999). Transforming properties of the Huntingtin interacting protein 1/ platelet-derived growth factor beta receptor fusion protein. J. Biol. Chem. *274*, 22328–22336.
24. Rao, D.S., Hyun, T.S., Kumar, P.D., Mizukami, I.F., Rubin, M.A., Lucas, P.C., Sanda, M.G., and Ross, T.S. (2002). Huntingtin-interacting protein 1 is overexpressed in prostate and colon cancer and is critical for cellular survival. J. Clin. Invest. *110*, 351–360.
25. Bazill, G.W., and Dexter, T.M. (1990). Role of endocytosis in the action of ether lipids on WEHI-3B, HL60, and FDCP-mix A4 cells. Cancer Res. *50*, 7505–7512.
26. Graeven, U., Rodeck, U., Karpinski, S., Jost, M., Philippou, S., and Schmiegel, W. (2001). Modulation of angiogenesis and tumorigenicity of human melanocytic cells by vascular endothelial growth factor and basic fibroblast growth factor. Cancer Res. *61*, 7282–7290.
27. Venkataraman, G., Sasisekharan, V., Herr, A.B., Ornitz, D.M., Waksman, G., Cooney, C.L., Langer, R., and Sasisekharan, R. (1996). Preferential self-association of basic fibroblast growth factor is stabilized by heparin during receptor dimerization and activation. Proc. Natl. Acad. Sci. USA *93*, 845–850.

28. Spivak-Kroizman, T., Lemmon, M.A., Dikic, I., Ladbury, J.E., Pinchasi, D., Huang, J., Jaye, M., Crumley, G., Schlessinger, J., and Lax, I. (1994). Heparin-induced oligomerization of FGF molecules is responsible fo FGF receptor dimerization, activation, and cell proliferation. Cell *79*, 1015–1024.
29. Kannan, K., Sharpless, N.E., Xu, J., O'Hagan, R.C., Bosenberg, M., and Chin, L. (2003). Components of the Rb pathway are critical targets of UV mutagenesis in a murine melanoma model. Proc. Natl. Acad. Sci. USA *100*, 1221–1225.
30. Halaban, R. (1999). Melanoma cell autonomous growth: the Rb/E2F pathway. Cancer Metastasis Rev. *18*, 333–343.
31. Choubey, D., and Gutterman, J.U. (1997). Inhibition of E2F–4/DP-1-stimulated transcription by p202. Oncogene *15*, 291–301.
32. Konduri, S., Lakka, S.S., Tasiou, A., Yanamandra, N., Gondi, C.S., Dinh, D.H., Olivero, W.C., Gujrati, M., and Rao, J.S. (2001). Elevated levels of cathepsin B in human glioblastoma cell lines. Int. J. Oncol. *19*, 519–524.
33. Eroglu, A., Toner, M., and Toth, T.L. (2002). Beneficial effect of microinjected trehalose on the cryosurvival of human oocytes. Fertil. Steril. *77*, 152–158.
34. Dudas, J., Ramadori, G., Knittel, T., Neubauer, K., Raddatz, D., Egedy, K., and Kovalszky, I. (2000). Effect of heparin and liver heparan sulphate on interaction of HepG2-derived transcription factors and their cis-acting elements: altered potential of hepatocellular carcinoma heparan sulphate. Biochem. J. *350*, 245–251.
35. Oelschlager, C., Romisch, J., Staubitz, A., Stauss, H., Leithauser, B., Tillmanns, H., and Holschermann, H. (2002). Antithrombin III inhibits nuclear factor kappaB activation in human monocytes and vascular endothelial cells. Blood *99*, 4015–4020.
36. Klein, M.D., Drongowski, R.A., Linhardt, R.J., and Langer, R.S. (1982). A colorimetric assay for chemical heparin in plasma. Anal. Biochem. *124*, 59–64.
37. Nugent, M.A., and Edelman, E.R. (1992). Kinetics of basic fibroblast growth factor binding to its receptor and heparan sulfate proteoglycan: a mechanism for cooperactivity. Biochemistry *31*, 8876–8883.
38. Padera, R., Venkataraman, G., Berry, D., Godvarti, R., and Sasisekharan, R. (1999). FGF-2/fibroblast growth factor receptor/heparin-like glycosaminoglycan interactions: a compensation model for FGF-2 signaling. FASEB J. *13*, 1677–1687.
39. van Kuppevelt, T.H., Dennissen, M.A., van Venrooij, W.J., Hoet, R.M., and Veerkamp, J.H. (1998). Generation and application of type-specific anti-heparan sulfate antibodies using phage display technology. Further evidence for heparan sulfate heterogeneity in the kidney. J. Biol. Chem. *273*, 12960–12966.
40. van de Westerlo, E.M., Smetsers, T.F., Dennissen, M.A., Linhardt, R.J., Veerkamp, J.H., van Muijen, G.N., and van Kuppevelt, T.H. (2002). Human single chain antibodies against heparin: selection, characterization, and effect on coagulation. Blood *99*, 2427–2433.